www.rericjournal.ait.ac.th

Phase Angle Based Control Strategy for Single-Stage Grid-Connected PV System

Muhammad Quamruzzaman[*1] and Kazi Mujibur Rahman[#]

Abstract *– This paper proposes a new phase angle based control strategy for a single-stage grid-connected PV system. The maximum power from the PV array was extracted adjusting phase angle of the inverter switching patterns only keeping modulation index constant. Conventional H-bridge voltage source inverter (VSI) in series with a line frequency transformer was used as power conditioning unit (PCU). The single stage power interface eliminated the need for the feedback control loops essential in a two-stage converter system to keep the dc link voltage constant for maintaining the power balance and thus the overall system operation was made more stable. Because of the nature of the control process some reactive power was also injected into the grid simultaneously depending on the PV array output and grid voltage condition. The proposed scheme features stable operation and better utilization of the PV array, reduced harmonics and lesser computations. Apart from modeling and analysis, detail simulation results are presented that demonstrates the effectiveness of the proposed technique.*

Keywords – Grid-connected photovoltaic (GCPV) system, modulation index, maximum power point tracking (MPPT), phase angle, single-phase photovoltaic (PV) inverter.

1. INTRODUCTION

The increasing energy consumption around the world has led to massive exhaustion of fossil-fuel reserves, disastrous carbon contamination and pollution, resulting global warming and weather change. There is a global demand for environment protection through using renewable energy resources instead of relying on fossil fuels. The solar energy in particular has drawn interest as a sustainable energy resource. Small scale use of solar photovoltaic (PV) modules for remotely located isolated users and large scale use of grid-connected PV's (GCPV) are both practiced worldwide.

GCPV systems are designed to operate in parallel with the electric utility grid. The primary component is the inverter, or power conditioning unit (PCU). The inverter converts the DC power produced by the PV array into AC power consistent with the voltage and power quality required by the utility grid. A bi-directional interface is made between the PV system AC output circuits and the electric utility network, typically at an on-site grid-connected distribution panel or service entrance. This allows the power produced by the PV system to either supply on-site electrical loads, or back feed the grid when the PV system output is greater than the on-site load demand. During periods when the PV generation is absent (night time) or less than the electrical demand of the on-site load, the balance of power required is received from the electric utility.

*Department of Electrical and Electronic Engineering, Chittagong University of Engineering and Technology, Pahartoli, Raozan, Chittagong-4349, Bangladesh.

[#]Department of Electrical and Electronics Engineering, Bangladesh University of Engineering and Technology, Dhaka-1000, Bangladesh.

[1]Corresponding author; Tel: +88-01713109848, Fax: + 88-02-9668054.
E-mail: qzaman359@yahoo.com.

1.1 Maximum Power Point Tracking (MPPT)

The output power of a PV array varies according to the sunlight conditions, atmospheric conditions, including cloud cover, local surface reflectivity, and temperature. Therefore, it is important to utilize it effectively and extract the maximum possible power from the PV array. The I-V and P-V characteristics of the PV array are nonlinear as shown in Figure 1 and the power extracted from it depends on its operating point. For a given irradiance (S) and temperature (T), there exists a single operating point corresponding to the maximum power point (MPP) of the PV array. As S and T vary, the corresponding MPP is tracked through using MPPT techniques.

MPPT is performed using the theory of maximum power transfer based on impedance matching. Maximum power from the PV array will be extracted when the load impedance presented to the PV array will be equal to its own impedance. Most GCPV systems have a DC-DC conversion interface followed by a DC-AC inverter. In most cases, the MPPT algorithm is implemented in the DC-DC converter stage [1]-[4]. The task of impedance matching is performed by adjusting duty cycle of the DC-DC converter.

There are three basic types of DC-DC converter: (1) buck converter (2) boost converter and (3) buck-boost converter. All these converters operate on the same basic principle. In Figure 2, Z_{in} is the Thevenin's equivalent impedance appearing at the PV array terminals. If D is the duty cycle, the expression of Z_{in} for different converters can be written as [5]:

$$\text{Buck:} \quad Z_{in} = Z_o \times (1/D)^2 \tag{1}$$

$$\text{Boost:} \quad Z_{in} = Z_o \times (1-D)^2 \tag{2}$$

$$\text{Buck-boost:} \quad Z_{in} = Z_o \times ((1-D)/D)^2 \tag{3}$$

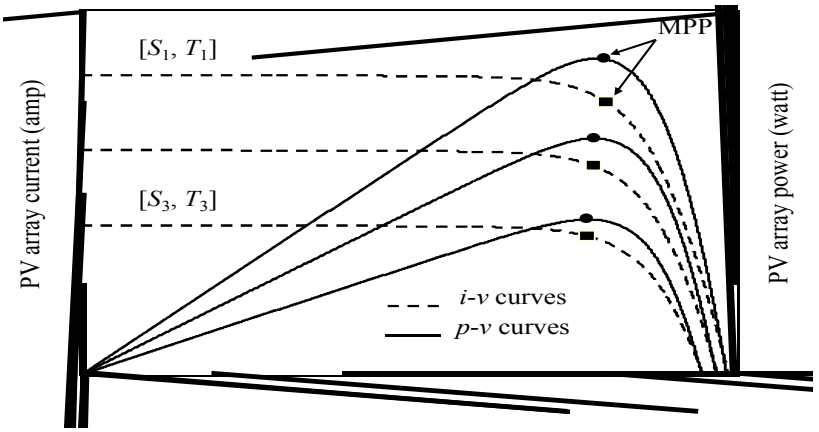

Fig. 1. I-V and P-V characteristics of PV panels under different irradiance and temperature conditions.

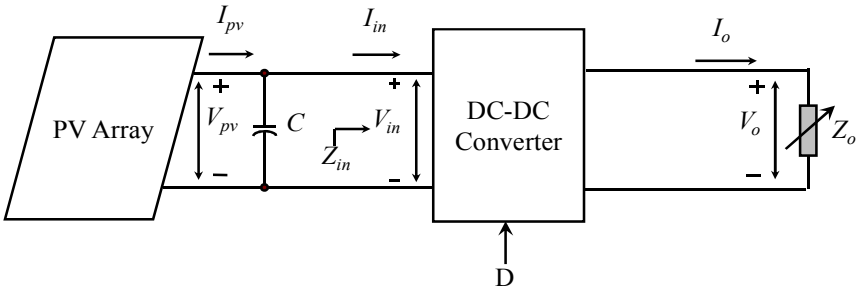

Fig. 2. MPPT using DC-DC converter.

1.2 GCPV System Topology

Various topologies for GCPV systems are found in the literature. The number of power conversion stages involved in a GCPV system is an important issue, as it determines the overall performance and system cost. Grid connected PV systems usually employ two stages for conditioning the available solar power for feeding into the grid [1]-[4]. Figure 3 shows a usual two-stage topology of GCPV system.

The first stage comprises DC-DC converter for boosting the array voltage and for MPPT. The high power application of this converter is limited for the following reasons:

- Switching losses are greater in high power applications that limit the switching frequency.
- The kVA rating of the inductor used in the converter is large. The size of the ferrite core required in the inductor becomes larger that increases cost.

Moreover, the large change in the output voltage of the boost converter for small adjustment of duty cycle increases the probability of unstable operation during closed loop control.

Power processing stages may be reduced by using an array providing large PV voltage. This can be realized using series connected modules followed by an H-bridge inverter [6], [7]. A PV array with large dc voltage suffers from drawbacks such as hot-spots during partial shading of the array, reduced safety and increased probability of leakage current through the parasitic capacitance between the panel and the system ground [8], [9]. Depending on the topology, switch states and environmental conditions the leakage current can cause electromagnetic (conducted and radiated) interference, distortion of the grid current and additional losses in the system. Measures to minimize leakage current are mentioned in [10]. There are also transformerless single-stage systems employing special type of boost inverters that perform boosting voltage, tracking MPP and dc-ac conversion [11]-[13]. The boost inverter is a special type of inverter consisting of two buck-boost converters connected back-to-back. This topology is not suitable for high power applications. Moreover, in such transformerless systems, there is more possibility of dc current injection into grid, which is undesirable [14].

Using transformer adds to the bulk of the system. Line frequency transformers are frequently used in power system and they can be designed for lesser losses and lower costs than DC-DC converters. Moreover, using line frequency transformers can facilitate the high power applications of the PV system. Therefore, if reliability and costs are rendered priority over bulk, the topology with transformer may be a good option. Figure 4 shows a single-stage GCPV system with transformer.

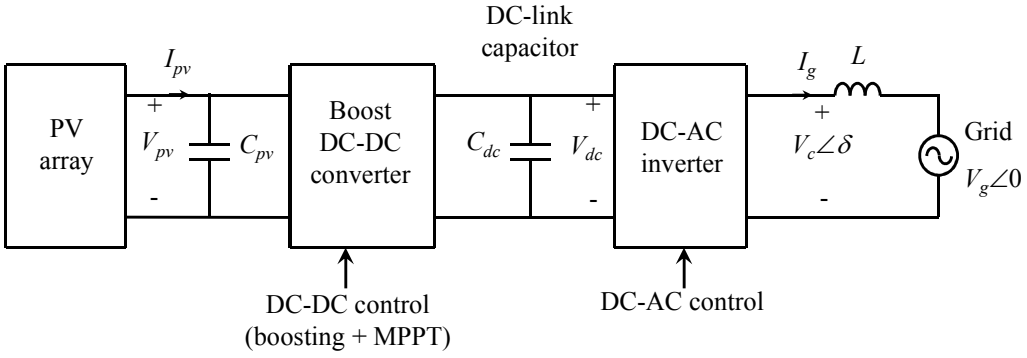

Fig. 3. Usual two-stage topology of grid-connected PV system.

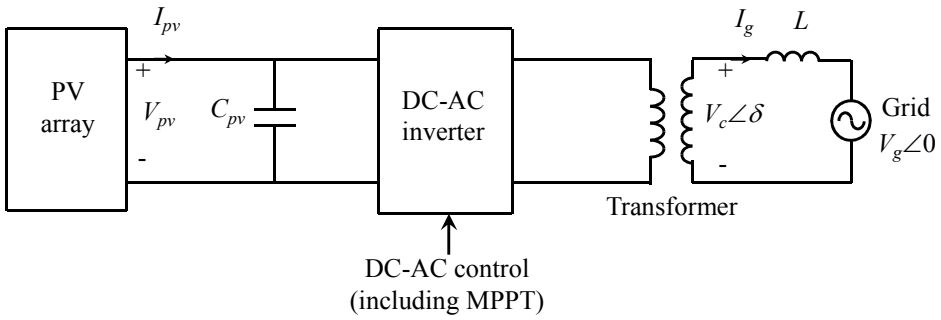

Fig. 4. Single-stage topology of grid-connected PV system with transformer.

1.3 Control Strategy of the GCPV System

As already stated in sec. 1.1, the maximum power from the PV array in most cases is extracted by adjusting the duty cycle of the DC-DC converter through using MPPT algorithm. In single-stage systems, MPPT is performed by adjusting modulation index of the inverter [11]. In the two-stage systems, extra control loops are employed to regulate the injected ac line current to keep dc-link voltage constant for balance between generated PV power and injected power into grid.

Most of today's GCPV systems employ current controlled voltage source inverters (CCVSI) [15] where inverter output current is regulated and injected into grid at unity power factor. In current control scheme, the instantaneous waveform of the current to be output is applied as the reference value. The switching device is turned on/turned off to change the output voltage so that the actual output current agrees with the current reference value within certain tolerance.

The control strategy based on adjustment of modulation index incurs some disadvantages. Figures 5 and 6 show the PWM patterns and corresponding frequency spectrums for different modulation indices (M) and constant phase angle (δ). It is found that decreasing modulation index decreases the magnitude of fundamental component but increases harmonics. Therefore, if the control strategy of the inverter is based on adjusting modulation index, it will incur following drawbacks:

- Decreasing M will increase harmonics that will result more losses.
- Voltage and current Total Harmonic Distortion (THD) will be increased.
- PWM pattern changes with the change of modulation index. Therefore, each time the modulation index is adjusted, PWM pattern needs to be recalculated and optimized which involves greater computational complexity and time. If the PWM patterns are calculated off-line, huge number of patterns needs to be stored, that increases memory requirements and cost. Therefore, it becomes difficult to implement the scheme with simple controller.
- Filter size will be larger since it is designed for the lowest value of M.

The DC link prior to inverter is a crucial point in GCPV systems as it leads to instability in case of improper power balance. Special control loops are adopted to keep the dc link voltage to constant value through using multiple feedbacks. Feedback systems because of extensive reliance on electronic hardware and sensing devices are prone to instability arising from failure of the control loops due to instrumental measurement error.

This paper has proposed a new phase-angle based control strategy for grid-connected PV system. Voltage controlled voltage source inverter (VCVSI) is used which is operated using pre-calculated optimized PWM patterns while tracking MPP by adjusting the phase

angle of the inverter output voltage with respect to the reference grid. The single stage power interface eliminates the need for the feedback control loops essential in a two-stage converter system to maintain the power balance and thus the overall system operation is made more stable. The modulation index of the inverter is kept constant at the highest possible value that ensures reduced harmonics lower current THD and lesser computations.

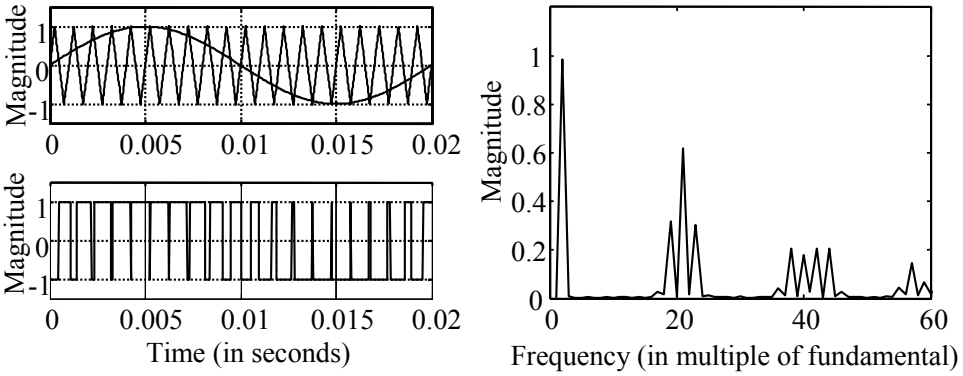

Fig. 5. PWM pattern and frequency spectrum for f =50 Hz, f_c = 1000 Hz, M = 1.0 and δ = 0^0.

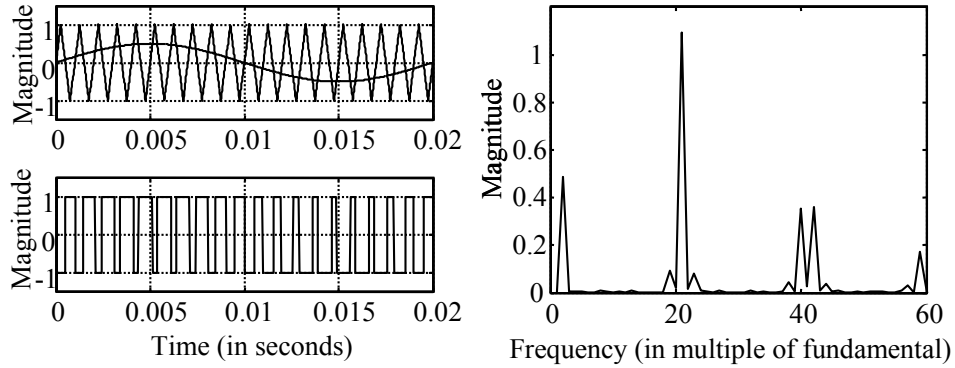

Fig. 6. PWM pattern and frequency spectrum for f =50 Hz, f_c = 1000 Hz, M = 0.5 and δ = 0^0.

2. AN ANALYSIS FOR MAXIMUM POWER TRANSFER: IMPEDANCE MATCHING USING DC-AC INVERTER

A single-stage grid-connected PV system is shown in Figure 7 where DC/DC converter is omitted and inverter is used for MPPT and DC/AC inversion. Here the task of impedance matching can be performed by adjusting modulation index (M) or phase angle (δ) of the inverter switching patterns as explained below:

$$\text{Inverter output voltage, } V_c = \frac{MV_{in}}{\sqrt{2}} \quad (4)$$

$$\text{Input power, } P_i = V_{in} I_{in} \quad (5)$$

$$\text{Output power, } P_o = \frac{V_c V_g}{X_L} \sin\delta \quad (6)$$

From Equations 4 to 6 we get,

$$V_{in} = \frac{\sqrt{2}\, V_c}{M} \quad (7)$$

$$I_{in} = \frac{M V_c}{\sqrt{2}\, X_L} \sin\delta \quad (8)$$

$$\therefore Z_{in} = \frac{V_{in}}{I_{in}} = \frac{2 V_c X_L}{M^2 V_g \sin\delta} \quad (9)$$

The coupling inductance L is constant and grid voltage V_g can be assumed constant. Varying either modulation index M or phase angle δ or both will vary Z_{in}. Therefore, task of impedance matching can be undertaken and thereby maximum power can be extracted adjusting either of these parameters or both simultaneously.

3. MODEL OF THE PROPOSED SCHEME

A model of the proposed scheme is shown in Figure 8. The simulink model of the scheme is given in Figure 9. The block called 1-phase inverter consists of the submodel (Figure 10) where the modulating signal for Sine Pulse Width Modulation (SPWM) is produced to generate PWM pulses. The 'Load' represents the total single phase load connected to grid. The phase shifting network and phase locked loop (PLL) is not included in the simulink model. For the simulation purpose with the simulink model, the switching patterns of the inverter are assumed to be synchronized with the grid. However, to make the scheme practically implementable, the

phase shifting network is designed in Pspice (Figure 11) to produce the phase shifted reference signal for PLL. Figures 12(a) – 12(d) show the grid reference and the phase shifted signals at different angles.

In Figure 11, the voltage applied to the inverting input of the comparator is varied by using variable resistor or Pot. During implementation of the scheme, the phase angle value (δ) modified by the MPPT algorithm may be converted to suitable voltage value that would produce the necessary phase shift (δ) of the reference voltage V_{ref}.

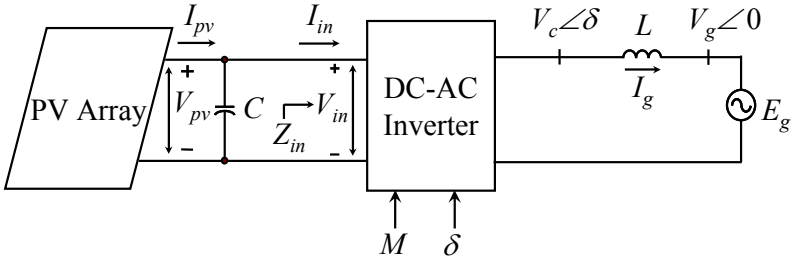

Fig. 7. MPPT using DC-AC inverter.

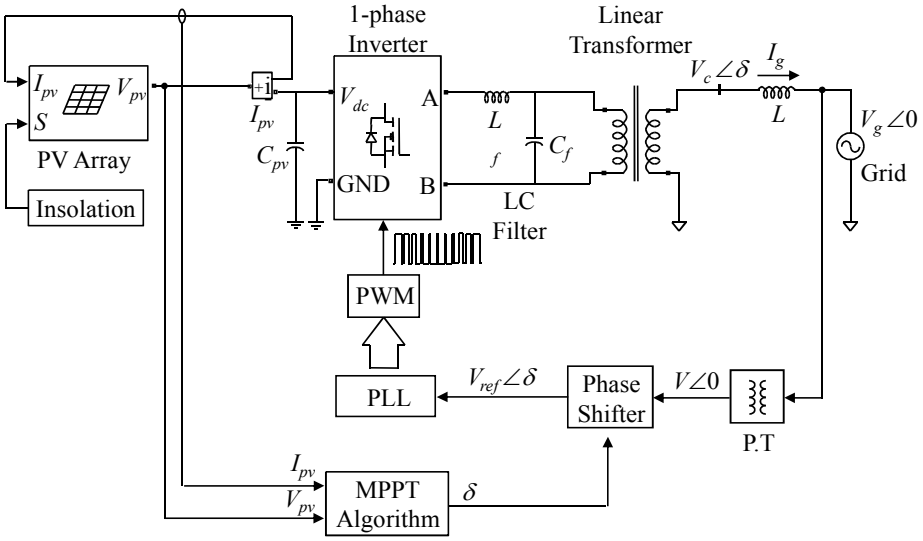

Fig. 8. Model of the proposed grid-connected PV system.

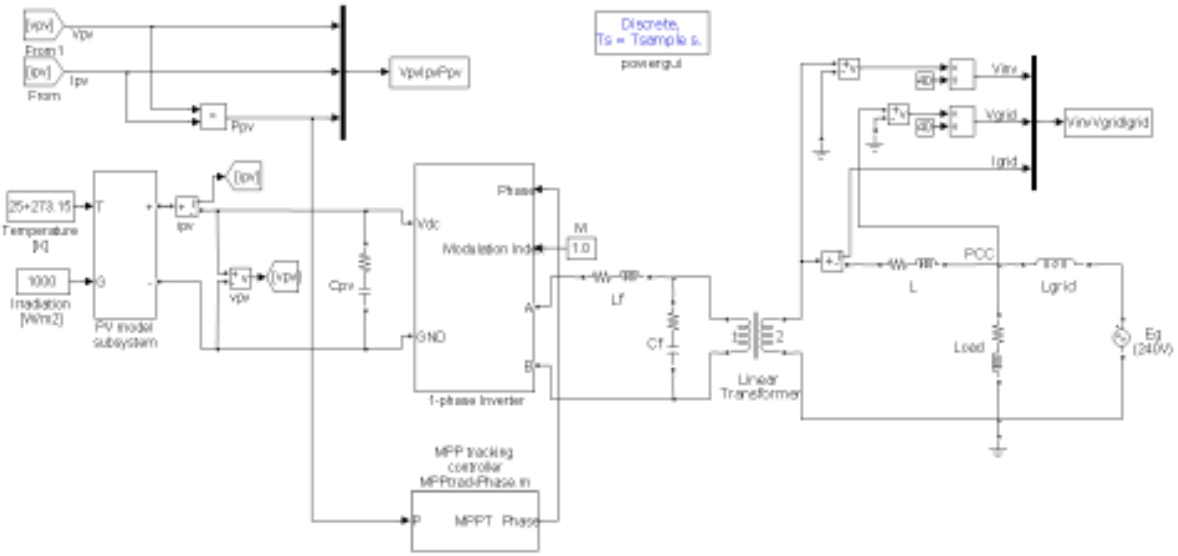

Fig. 9. Simulink model of the scheme.

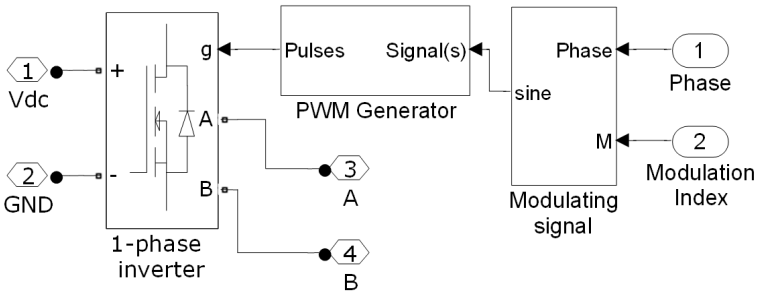

Fig. 10. 1-phase inverter block.

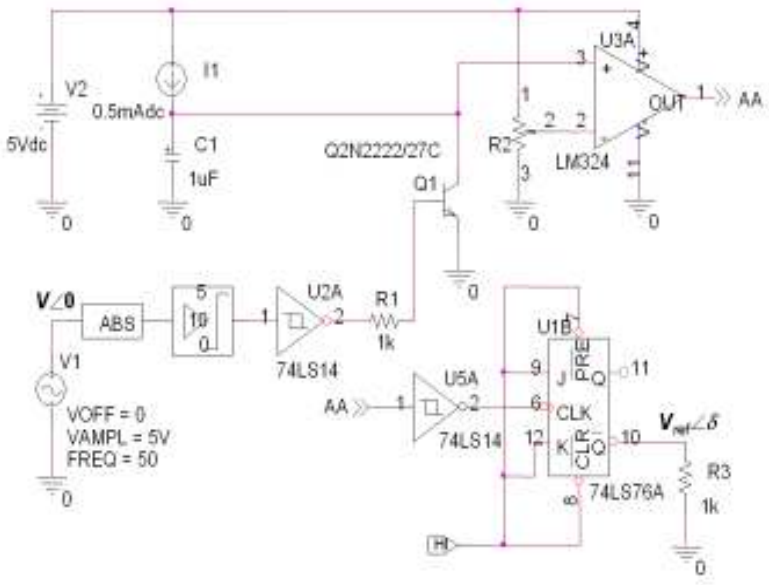

Fig. 11. Phase shifting circuit.

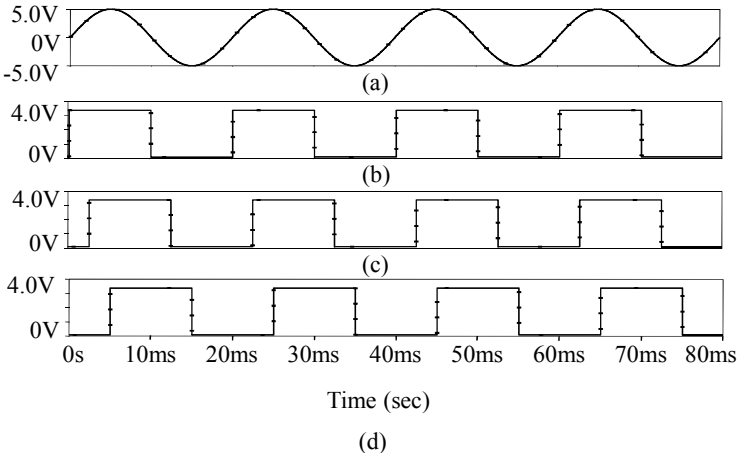

Fig. 12. (a) Grid voltage reference, $V\angle 0^0$ (b) $V_{ref}\angle 0^0$ (c) $V_{ref}\angle 45^0$ (d) $V_{ref}\angle 90^0$.

4. MAXIMUM POWER POINT TRACKING

To find the MPP at all conditions, the MPPT control method based on perturb-and-observe (P and O) algorithm was adopted owing to its simple structure and the fact that it requires fewer measured parameters. Since P and O algorithm is well known and widely used, it is not going to be explained in full detail. Only the phase angle of the PWM switching signal for inverter is modified by the MPPT algorithm for attaining the MPP.

The performance of the MPPT algorithm greatly depends on the step-size chosen. Larger step-size results greater oscillations around MPP. Smaller step-size reduces oscillations but makes the process slower. For a solution to this conflicting situation, a variable perturbation size was adopted. The initial step-size ($d\delta$) was assumed larger and as the operating point approached MPP, the step-size was gradually lowered to ensure faster convergence and less oscillations. The

process of adopting variable step-size is explained below.

The power versus phase angle curves (Figure 13) at different irradiances are obtained through simulation adjusting the phase angle manually. It has been found that the derivative $d\varphi_{k\max} / dP_{k\max}$ is almost constant.

$$\frac{\varphi_{1\max}-\varphi_{2\max}}{P_{1\max}-P_{2\max}} \cong \frac{\varphi_{2\max}-\varphi_{3\max}}{P_{2\max}-P_{3\max}} \cong .... \frac{\varphi_{k\max}-\varphi_{(k+1)\max}}{P_{k\max}-P_{(k+1)\max}}$$

It has been noticed while performing simulation that whenever change of irradiance occurs, the PV array power (vs. time) curve, before being stable around the MPP, crosses a point where the value of power is equal to the maximum value of power corresponding to the changed irradiance. In each case of irradiance change, it is found that the PV power curve attains a maximum value $P_{max\_initial}$ shortly after the change of irradiance before reaching the actual stable maximum power point P_{max_stable} (Figure 14). Thus, the information of the maximum attainable power P_{kmax} can be obtained at the very beginning of the changed conditions that can be used to determine an approximate phase angle (φ_{kmax}) corresponding to MPP.

When φ_{kmax} is determined, the step-size can be calculated as

$$\Delta\varphi_k = (\varphi_{k\max} - \varphi)/\beta \quad (10)$$

where, β is a constant. Since the difference ($\varphi_{kmax} - \varphi$) decreases as the operating point approaches MPP, the step size gradually becomes smaller.

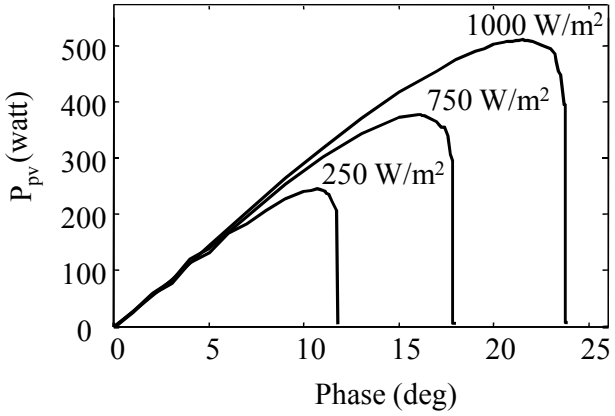

Fig. 13. PV power versus phase angle curves.

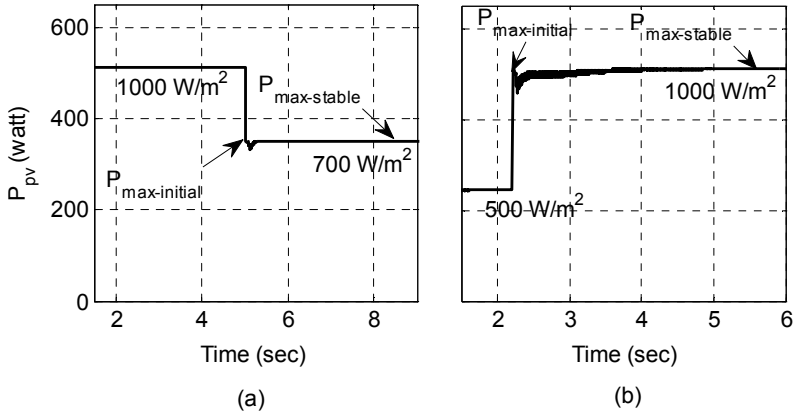

Fig. 14. PV power curves for irradiance changes from (a) 1000 W/m^2 to 700 W/m^2 and (b) 500 W/m^2 to 1000 W/m^2.

Figures 15(a) – (c) show how the oscillations around MPP decreases at the cost of convergence speed with the reduction of step-size. Figure 15(d) shows that with the proposed method the oscillations around MPP decreases as well as convergence speed increases.

The oscillations at 1000 W/m^2 are shown more precisely in Figures 16(a) – 16(d). In Figures 16(a) – 16(c) it is seen that when fixed step-size is employed, less oscillation occurs for smaller step-size. Oscillation is minimum for variable step-size with the proposed method as seen in Figure 16(d). Thus, the proposed modified method with variable step-size reveals better performance.

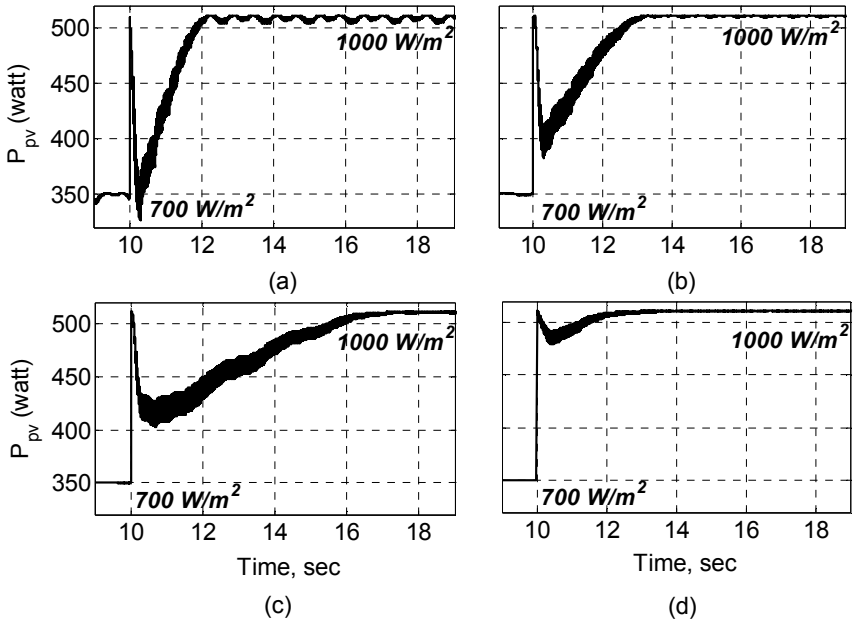

Fig. 15. PV array power for irradiance changes from 700 W/m^2 to 1000 W/m^2 when perturbation step-size is (a) 1.0 (b) 0.5 and (c) 0.2 and (d) variable according to the proposed method.

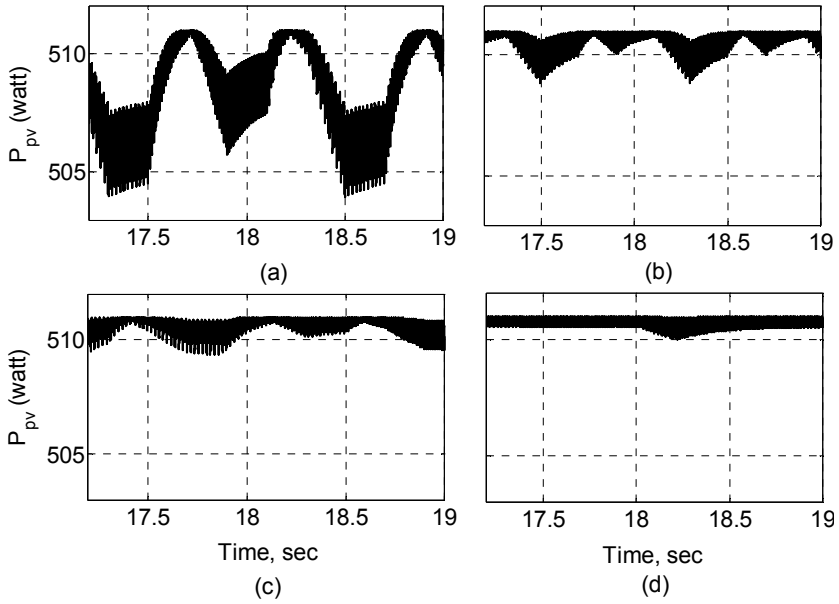

Fig. 16. Oscillations in PV array power at irradiance 1000 W/m^2 when perturbation step-size is (a) 1.0 (b) 0.5 and (c) 0.2 and (d) variable according to the proposed method.

5. SIMULATION RESULTS

The proposed phase angle based scheme was simulated using matlab and simulink. The circuit parameter values used in the simulation are listed in Table 1. The rating of the PV array used in the simulation is given in Table 2 (at standard testing conditions i.e. 1000W/m^2 irradiance and 25^{0}C temperature). The parameters for different solar irradiances found through simulation are listed in Table 3. The transformer used was assumed ideal with the turns ratio 1:4.

The scheme was simulated without considering any on-site load. The phase angle of the inverter switching pattern was adjusted and MPP was tracked at different irradiance conditions as shown in Figure 17. The modulation index was maintained constant at 1.0.

It was found that at the irradiance values 1000 W/m^2, 700 W/m^2, 600 W/m^2 and 500 W/m^2 the average power extracted from the array were 510.8 W, 350.5 W, 297.65 W and 245 W respectively, which were very close to the values given in Table 2 and Table 3. The variation of instantaneous PV power was only 0.03 W – 0.3 W. Thus, the MPPT algorithm was proved to perform very well.

Table 1. Parameters used in the simulation

C_{pv}	L_f	C_f	L	L_{grid}
10mF	10mH	10μF	10mH	0.01mH

Table 2. PV array rating (at standard testing conditions).

Symbol	Parameter	Value
I_{sc}	Short-circuit current	5.42 A
V_{oc}	Open-circuit voltage	133.2 V
P_{max}	Maximum PV power	511 W
V_{pmax}	Voltage at maximum power	103.6 V
I_{pmax}	Current at maximum power	4.93 A

Table 3. PV array characteristics at different irradiances.

Irradiance (W/m^2)	V_{pmax} (V)	I_{pmax} (A)	P_{max} (W)
700	101.5	3.45	350.7
600	100.5	2.96	297.7
500	98.46	2.49	245.1

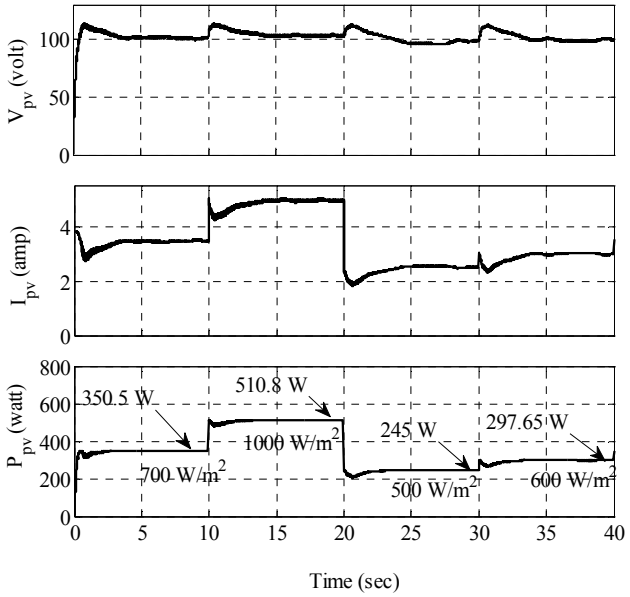

Fig. 17. PV array voltage, current and power under different irradiance conditions.

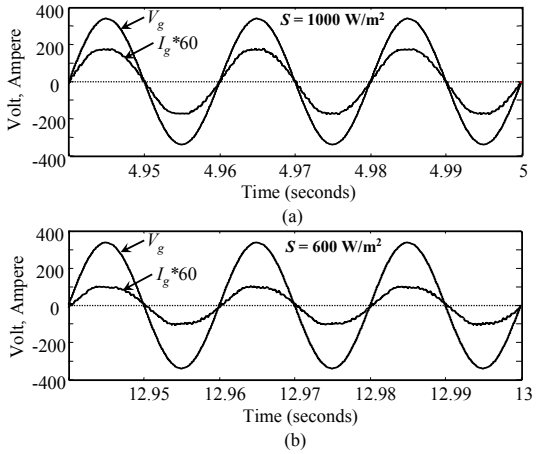

Fig. 18. Inverter output voltage, Grid voltage and current injected into grid when V_g=240V and solar irradiance is (a) 1000 W/m^2, (b) 600 W/m^2.

The waveshapes of inverter output voltage, grid voltage and current injected into grid are shown in Figure 18. Similar results are shown in Figure 19 for grid voltage reduced to 210V. When the grid voltage was 240V, the inverter injected current at a power factor close to unity and the amount of reactive power injection into grid was negligible. As the grid voltage decreased to 210V, the current injected into grid became more lagging and the reactive power injection into grid increased considerably.

Figure 20 shows the amount of reactive power injected into grid when maximum power was extracted from the PV array and delivered to grid at different irradiance conditions. Reactive power injection was negligible for 240V, the nominal value of grid voltage. Further, the PV inverter injected considerable amount of reactive power into grid when grid voltage was lowered to 210V. Thus, the proposed scheme helps in grid power conditioning.

The frequency spectrum of the current injected into grid and the percentage of different harmonics in the grid current for irradiance 1000W/m^2 are shown in Figures 21(a) and 21(b), respectively. The current THD obtained was 3.6%. It is seen that current THD and individual harmonic components are sufficiently less and within the limit specified in IEC 61727 [16].

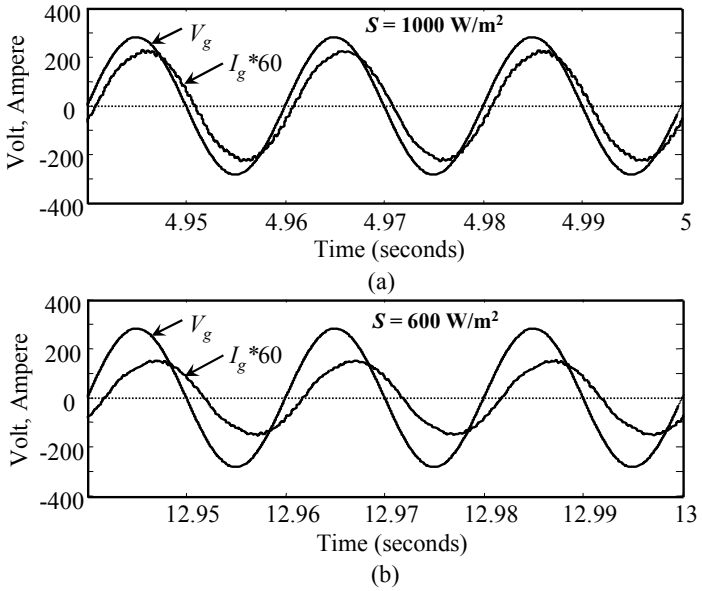

Fig. 19. Inverter output voltage, grid voltage and current injected into grid when V_g=210V and solar irradiance is (a) 1000 W/m^2, (b) 600 W/m^2.

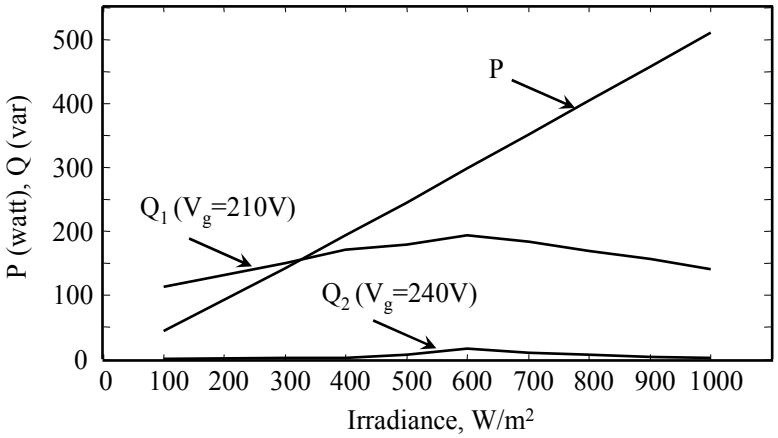

Fig. 20. Active power and reactive power supplied by the PV inverter at different irradiance conditions and grid voltages.

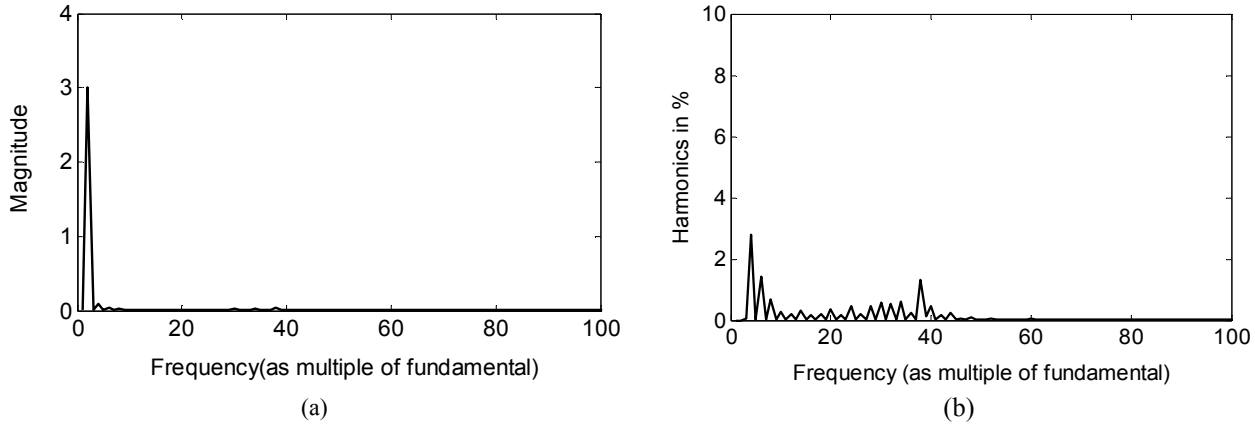

Fig. 21. (a) Frequency spectrum of the current injected into grid (b) percentage of different harmonic components in the grid current.

5. CONCLUSION

A novel control strategy for grid-connected PV system based on phase angle adjustment has been presented in this paper. The MPPT algorithm that adjusted only the phase angle of the inverter switching patterns keeping modulation index constant could track changes in solar irradiation. The oscillations around MPP was reduced and convergence speed increased considerably by adopting variable step-size with the approximation of phase angle at MPP at any irradiance. The control strategy was tested with varying irradiances and was found to offer stable operation. Omission of DC-DC converter and use of line frequency transformer has made the scheme suitable for low, medium and high power applications. Furthermore, the proposed control strategy eliminates the need for the feedback control loops for keeping the inverter input voltage constant and thus makes the system operation more stable. It is shown that the PV inverter can inject considerable amount of reactive power into grid when grid voltage deteriorates. Due to constant modulation index, the proposed scheme has the desirable features such as reduced harmonics and less computation.

REFERENCES

[1] Mekhilef, S., 2008. Performance of grid connected inverter with maximum power point tracker and power factor control. *International Journal of Power Electronics* 1(1): 49-62.

[2] Hassaine, L., Olias, E., Quintero, J. and Haddadi, M., 2009. Digital power factor control and reactive power regulation for grid-connected photovoltaic inverter. *Renewable Energy* 34(1): 315-321.

[3] Albuquerque, F.L., Moraes, A.J., Guimaraes, G.C., Sanhueza, S.M.R. and Vaz, A.R., 2010. Photovoltaic solar system connected to the electric power grid operating as active power generator and reactive power compensator. *Solar Energy* 84(7): 1310-1317.

[4] Chen, Y.-M., Wu, H.-C., Chen, Y.-C., Lee, K.-Y. and Shyu, S.-S., 2010. The AC line current regulation strategy for the grid-connected PV system. *IEEE Transactions on Power Electronics* 25(1): 209–218.

[5] Jain, S. and V. Agarwal, 2007. New current control based MPPT technique for single stage grid connected PV systems. *Energy Conversion and Management* 48(2): 625-644.

[6] Liang, T.J., Kuo, Y.C. and Chen, J.F., 2001. Single-stage photovoltaic energy conversion system. *IEE Proceedings on Electric Power Applications* 148(4): 339-344.

[7] Chen, Y. and K. Ma-Smedley, 2004. A cost-effective single-stage inverter with maximum power point tracking. *IEEE Transactions on Power Electronics* 19(5): 1289–1294.

[8] Blaabjerg, F., Chen, Z. and Kjaer, S.B., 2004. Power electronics as efficient interface in dispersed power generation systems. *IEEE Transactions on Power Electronics* 19(5): 1184–1194.

[9] Kjaer, S.B., Pedersen, J.K. and Blaabjerg, F., 2005. A review of single-phase grid-connected inverters for photovoltaic modules. *IEEE Transactions on Industry Applications* 41(5): 1292–1306.

[10] Su, N., Xu, D. and Tao, J., 2010. Ground current suppression for grid connected transformerless PV inverter with unbalanced output filter inductors. In *IEEE Energy Conversion Congress and Exposition*. Atlanta, Georgia, 12-16 September, 2010, pp. 3247 - 3252.

[11] Jain, S. and V. Agarwal, 2007. A single-stage grid connected inverter topology for solar PV systems with maximum power point tracking. *IEEE Transactions on Power Electronics* 22(5): 1928–1940.

[12] Lacerda, V.S., Barbosa, P.G. and Braga, E., 2010. A single-phase single-stage, high power factor grid-connected PV system, with maximum power point tracking. *IEEE International Conference on Industrial Technology*. Vina Del Mar, Chile, 14-17 March.

[13] Patel, H. and V. Agarwal, V., A Single-Stage Single-phase transformer-less doubly grounded grid-connected PV interface. *IEEE Transactions on Energy Conversion* 24(1): 93-101.

[14] Utility Aspects of Grid Connected Photovoltaic Power Systems, Std. IEA PVPS V-2-01, 1998.

[15] Ko, S.-H., Lee, S.-R., Dehbonei, H. and Nayar, C.V., 2006. Application of voltage- and current-controlled voltage source inverters for distributed generation systems. *IEEE Transactions on Energy Conversion* 21(3): 782-792.

[16] IEC 61727. 2004. Photovoltaic (PV) systems – Characteristics of the utility interface, 2nd Edition.